Eur. Phys. J. D **23**, 257–264 (2003)
DOI: 10.1140/epjd/e2003-00056-2

THE EUROPEAN PHYSICAL JOURNAL D

Two-photon laser-induced fluorescence of H_2O and D_2O molecules at ambient pressure

F. Edery and A. Kanaev[a]

Laboratoire d'Ingnierie des Matriaux et des Hautes Pressions, CNRS, Institut Galile, Universit Paris-Nord, 93430 Villetaneuse, France

Received 25 January 2002 / Received in final form 27 May 2002
Published online 4 March 2003 – © EDP Sciences, Società Italiana di Fisica, Springer-Verlag 2003

Abstract. We have carried out experiments of two-photon excitation of vapor phase H_2O and D_2O molecules at atmospheric pressure. A narrow-band tunable UV OPO laser is used in the experiments. Transient $\tilde{C}^1B_1 \rightarrow \tilde{A}^1B_1$ emission from the excited predissociating state is seen in both cases. The complete $\tilde{C}^1B_1 \leftarrow \tilde{X}^1A_1$ fluorescence excitation spectrum in the spectral range of 245–250 nm is measured and compared with theory. It is shown that the predissociation rate increases with the rotational quantum number $K'_a > 2$ more strongly than with K'^2_a. No perturbation effects on the measured LIF spectra are observed at a laser power density below 2 GW/cm^2. Experimental results indicate a negligible contribution from both molecular association and collisions with atmospheric gases. Only an extremely weak vibrational progression belonging to the second positive system of N_2 has been observed, which appears to be due to energy and charge transfer in $N_2^{+*} + H_2O$ collisions.

PACS. 33.80.Rv Multiphoton ionization and excitation to highly excited states (e.g., Rydberg states) – 32.50.+d Fluorescence, phosphorescence (including quenching) – 33.70.Fd Absolute and relative line and band intensities

1 Introduction

The water molecule has been considered for a long time as a good model system for both theoretical and experimental studies. Main features of water molecule spectroscopy have been explicitly outlined by Dutuit *et al.* [1]. The H_2O molecule is transparent in the UV-visible spectral range. Below the ionization limit at ∼12.6 eV it rapidly dissociates into the radical and the hydrogen atom in the ground state. The first absorption continuum at ∼160 nm has been extensively used in studies of the dissociation dynamics of free molecules [2] and those trapped in solid matrices [3]. Moreover, at excitation above 9.136 eV (135.71 nm) the excited product $OH^*(A^2\Sigma^+)$ appears in the decay channel with a quantum yield between 5 and 10%, allowing use of sensitive photofragment fluorescence techniques. A sketch of the relevant potential curves of the water molecule is presented in Figure 1.

Except for continua, earlier assigned to transitions to nsa_1 repulsive Rydberg states, absorption spectrum shows structured bands; the first member of these series is situated at ∼124 nm ($3pa_1 \leftarrow 1b_1$). These structures are associated with excitation of bound Rydberg states. Despite the fact that H_2O is a polyatomic molecule and the bound states rapidly predissociate, the rotational structure of the bound-bound transitions is partially resolved: the absorption spectrum exhibits oscillatory structure due to many overlapping bands [4].

Due to their low spectral intensity, the use of the synchrotron radiation or conventional spectroscopic lamps does not allow use of fluorescence techniques for analysis of predissociation dynamics with rotational state resolution. Commercial tunable lasers in the VUV spectral region are not available but, over the last two decades, a technique of multiphoton laser-induced fluorescence has attracted much attention for studies of simple molecules [5]. The H_2O molecule has been a subject of studies with two and three photon excitation on the $\tilde{C}^1B_1 \leftarrow \tilde{X}^1A_1$ transition (∼10 eV) [6–8]. Theoretical formalism supporting these studies has been developed by Dixon *et al.* [9]. Analysis has shown coupling of the lowest bound $\tilde{C}^1B_1$ state with the $\tilde{B}^1A_1$ repulsive state, the strength of which is a sensitive function of $\langle J'^2_a \rangle$, the mean square rotational angular momentum projection on the molecular axis a (the axis associated with the smallest moment of inertia). Moreover, two-photon LIF studies have enabled discovery of an extremely low-intensity transient fluorescence of H_2O and D_2O molecules, which appears following the excitation and during the predissociation process [10]. The use of this short-lived visible emission at 420 nm (assigned

[a] e-mail: kanaev@limhp.univ-paris13.fr

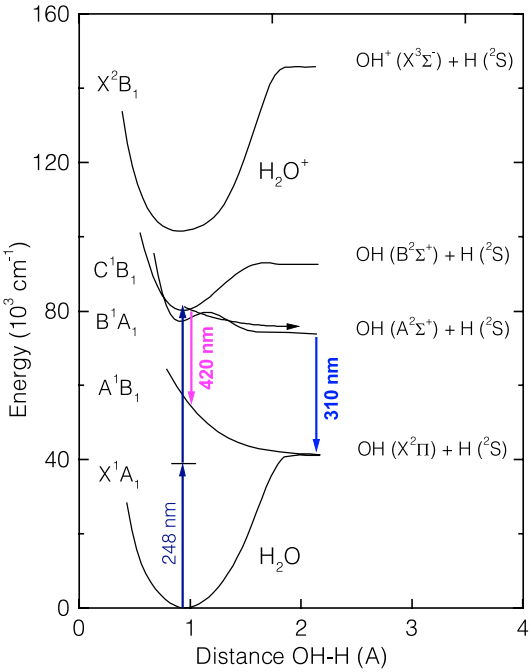

Fig. 1. A sketch of the relevant potential curves of the water molecule (HÔH $\sim 104°$).

to $\tilde{C}^1B_1 \rightarrow \tilde{A}^1B_1$ transition) has been suggested for LIF measurements of the temperature in gases at high pressures [11]. In particular, the $\tilde{C}^1B_1 \leftarrow \tilde{X}^1A_1$ excitation spectrum of OH($A \rightarrow X$) fluorescence was later used for a temperature evaluation of water molecules embedded in large helium clusters [12].

In all earlier studies, two-photon excitation spectra of H_2O and D_2O molecules were measured using a tunable KrF excimer laser in the range between 247.8 and 248.8 nm. Complete excitation spectra of these molecules are predicted to be broader and lie between 245 and 250 nm. Therefore, many strong spectral features may fall beyond the range of the laser tunability. Experimental analysis of the complete spectrum could be of importance for a refinement of molecular dynamics simulation techniques.

In the present study we report the analysis of the complete two-photon $\tilde{C}^1B_1 \leftarrow \tilde{X}^1A_1$ excitation spectra of H_2O and D_2O molecules ($\tilde{C}^1B_1 \rightarrow \tilde{A}^1B_1$ fluorescence). Moreover, the realization of temperature measurements at high pressures requires understanding of the effect of the environment on the involved electronic states and, in particular, the influence of quenching. Following this objective, we conducted the present experiments at ambient pressure. The short picosecond lifetimes of the excited state levels allow our use of this approach.

2 Experiment

Experiments were carried out using the pulsed nanosecond MOPO laser (*Spectra Physics*) tunable over the spectral range 0.22–1.7 μm. The laser delivers energy of $\sim$10 mJ/pulse in the spectral range of interest, 245–250 nm, with a repetition rate of 10 Hz. The spectral width of the laser line and the accuracy of the reproducibility of the laser frequency are $\sim$0.2 cm^{-1}. The pulsed laser energy is permanently monitored by a two-channel LabMaster (*Coherent*) energy meter. A quartz lens (f = 20 or 15 cm) focused the output laser beam into a windowless cylindrical cell through spatial filters, which allowed suppression of the background visible radiation. The use of this cell allows one to avoid the contamination of the weak measured spectra by parasite fluorescence from the supporting optical elements. Fluorescence from the region near the focal point was collected by a 400 μm UV-grade optical fiber 20-m long and oriented at a right angle to the laser beam. When the sample zone is illuminated, the fiber is not exposed directly to the laser radiation. Taking into account the acceptance angle of the fiber and its distance from the optical axis of the laser beam, the spatial resolution was estimated as $\leq$1.0 mm. Because of the length of the fiber, the scattered light of the pump radiation at $\lambda < 250$ nm is internally attenuated, facilitating observation of a weak fluorescence signal with $\lambda \geq 300$ nm.

The fiber transmits the fluorescence signal to a UV-visible monochromator (grating 150 l/mm, f = 30 cm, slit 20 μm) coupled to a CCD detector (*Princeton*). The signal is also sent to a H-20 filter-monochromator (*Jobin Yvon – Spex*) equipped with a fast and fully integrated photomultiplier (*Hamamatsu*). The cooled intensified CCD detector allows measurements of spectra with a time window $\Delta t \geq 5$ ns adjustable with in 1 ns steps with respect to the pump laser pulse. For the present experiments the time window has been synchronized to the excitation pulse. The photomultiplier signal is displayed by a 500 MHz TDS510 digitizing oscilloscope (*Tektronix*), which enables waveform analysis and fluorescence excitation spectra measurements.

In the high-resolution measurements of two-photon excitation spectra of H_2O and D_2O molecules, the fluorescence waveform from the digitizing oscilloscope is integrated in time, normalized to the mean squared laser intensity $\langle I_L^2 \rangle$ and stored in the PC computer. Typically, averaging of the signal over 10^2 laser shots was used in the current experiments for each excitation wavelength $\lambda_{\rm exc}$, which was scanned with an increment of $\leq$0.01 nm in the 245–250 nm spectral region. The filter-monochromator is fixed during these measurements at the maximum of the fluorescence band of interest.

High purity water and heavy water (99.998%), used in the present experiments, evaporate directly into the open cell. Additionally, the quality of the samples used in this work has been verified by Raman spectroscopy. Characteristic vibrational bands of pure H_2O at 1 650 and 3 300 cm^{-1}, and pure D_2O at 1 200 and 2 450 cm^{-1} dominated the spectra. No mixed (HDO) or impurity bands were observed in the tested liquids. In some experiments the cell was continuously flushed by a high purity nitrogen or argon gas flow. This sweeps away water molecules and

decreases the useful fluorescence signal (which reached a maximum at a saturation vapor pressure), but facilitates our assignment of the observed spectra.

3 Results and discussion

3.1 Fluorescence spectra

Observation of water vapor blue fluorescence is not a simple matter because of the very low quantum yield $q_{\rm vis}$. A rapid spontaneous predissociation of the excited state sets its lifetime $\tau^* < 10^{-11}$ s. Lifetimes of $\tau_C^* \sim 2.5$ ps and ~6 ps were estimated correspondingly for the $\tilde{C}$-state ($\nu' = J' = 0$) of H_2O and D_2O [6]. The rate of the $\tilde{C}^1B_1 \rightarrow \tilde{A}^1B_1$ fluorescence transition is $r \leq 10^8$ s^{-1}, and we can infer that $q_{\rm vis} = r\tau^* < 10^{-3}$. Secondly, the excited state undergoes ionization under powerful optical pumping. This partially explains why experiments with broadband excimer laser excitation failed to observe the parent fluorescence [13]. Apparently, for the same reason, non-reliable results were obtained in references [8,10] when observing fluorescence from the focal point region using a narrow-band KrF excimer laser. By excitation of water vapor with a lens of 15 or 20 cm focal length, we have observed the brightest fluorescence from the focal point region. Because the intensity of this fluorescence grows with water vapor pressure, we used a saturated pressure of ~24 mbar at a room temperature of 25 °C. Typical wavelength-resolved fluorescence spectra are shown in Figure 2. Figure 2a presents fluorescence from atmospheric gases. In Figure 2b the difference spectrum of fluorescence in presence of water vapor (minus the spectrum of Fig. 2a) is displayed. No appreciable changes were observed if we used a nitrogen gas flow. Therefore, we concluded that the main features are due to the presence of N_2 and H_2O molecules. For comparison in Figure 2c we show a fluorescence spectrum observed with a continuous argon gas flow.

The UV band at ~315 nm belongs to the $A^2\Sigma^+ \rightarrow X^2\Pi$ transition of OH, produced *via* predissociation of water molecules following absorption of two (or more) UV photons. Our low spectral resolution does not allow resolution of the rotational structure of this transition. The photofragment fluorescence quantum yield at 10 eV excitation is ~10% [14], which is much higher than the yield of transient fluorescence from the parent molecular water. Nevertheless, the intensities of these radiative transitions in Figure 2 are comparable. This could be due to a quenching of the long-lived OH($A^2\Sigma^+$) state emission, $\tau_A^* \approx 0.8$ μs ($\nu' = 0, 1$) [15], and its ionization in the laser field. Losses due to excited molecules escaping the fluorescence detection zone ($D \sim 1$ mm) can be disregarded because their time-of-flight $t_{\rm tfl} = D/V_{\rm OH^*}$ is smaller than the excited state lifetime τ_A^*. Indeed, the nascent velocity of the OH$^*(A)$ fragment ($V_{\rm OH^*}$) can be estimated from energy considerations. The gas phase dissociation energy of $H_2O(\tilde{X}) \rightarrow OH(X) + H$ is $D_e = 5.118$ eV and the transition energy of $OH(A \rightarrow X)$ is $T_e = 4.053$ eV. Therefore,

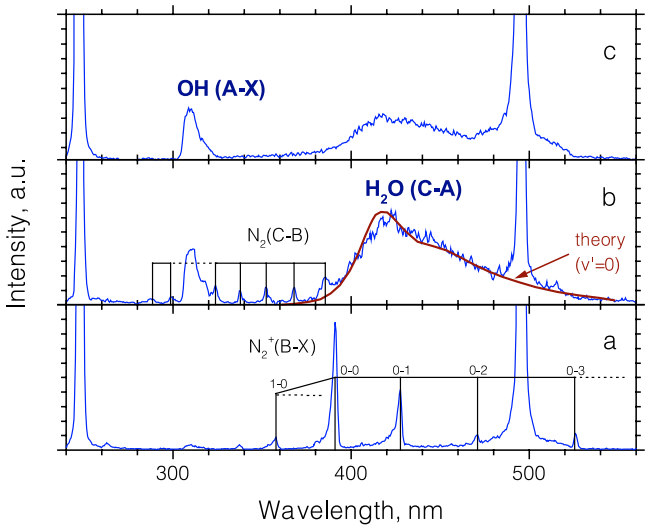

Fig. 2. Fluorescence spectra of: atmospheric air (a), difference spectrum of fluorescence in the presence of water vapor (minus the spectrum "a") (b), and water vapor under argon gas flow (c). Strong features at ~248 and ~496 nm are due to scattered laser radiation. The excitation wavelength is 247.910 nm; the laser power density is ~1.0 GW/cm^2. Partial emission cross-section for the OH($\nu' = 0$) vibrational channel from [10] is shown in (b) by the solid line.

the energy released in the reaction

$$H_2O + 2h\nu \rightarrow H_2O(\tilde{C}) \rightarrow OH(A) + H$$

is $2h\nu - D_e - T_e \approx 0.83$ eV. It is mainly distributed between rotational (OH) and translational (H) degrees of freedom. The centre-of-mass kinetic energy of OH$^*(A)$ is then 25 meV, which corresponds to a velocity of $V_{\rm OH^*} \sim 5 \times 10^4$ cm/s. We finally obtain $t_{\rm tfl} \approx 2$ μs $< \tau_A^* \approx 0.8$ μs.

We will make now estimates of the influence of quenching. If we assume that the main quenching agent is water vapor, than the fluorescence yield of OH$^*(A)$ can be estimated from $q_{\rm uv}^{(Q)} = \tau/\tau_A^* = 1/(\sigma_q V_{\rm OH^*}[H_2O]\tau_A^* + 1)$. Bailey *et al.* [16] have recently proposed describing the temperature dependence of the quenching cross-section by $\sigma_q(\text{Å}) = 20.847(1 + 440.82/T(1 + 271.77/T))$. Assuming the translational temperature of the OH$^*(A)$ fragment is $T \approx 300$ K (which corresponds to $V_{\rm OH^*} \sim 5 \times 10^4$ cm/s), one obtains the quenching cross-section $\sigma_q = 79$ Å^2 and $q_{\rm uv}^{(Q)} \approx 5 \times 10^{-3}$. The quenching of OH$^*(A)$ by nitrogen and argon gases at atmospheric pressure and, may be, by traces of O_2 and CO_2 result in a similar or weaker effect on $q_{\rm uv}^{(Q)}$ (see Ref. [17] and references therein). A comparison of the UV and visible continua (with $q_{\rm vis} = \tau/\tau_C^*(H_2O) \leq 2.5 \times 10^{-4}$) in Figures 2b and 2c allows estimating the experimental value of the UV fluorescence yield $q_{\rm uv}$. For the present experiments involving nitrogen and argon atmospheres, the value of $q_{\rm uv}$ is found to be a factor of ~10^2 lower than the estimated value $q_{\rm uv}^{(Q)}$ due to the quenching. Therefore, we can neglect the quenching, and we believe that in our experimental conditions losses of the excited

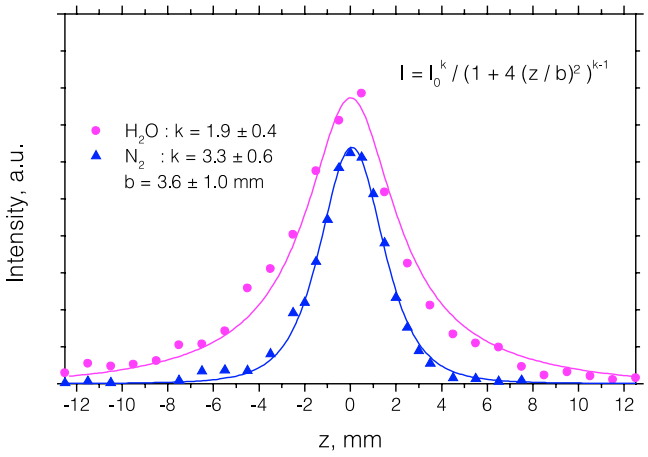

Fig. 3. Distribution of the fluorescence intensity of H_2O (420-nm continuum) and of H_2^+ (390-nm line) along the focal point ($f = 15$ cm). The excitation wavelength is 247.910 nm; laser power density at the focal point is ∼2.0 GW/cm^2.

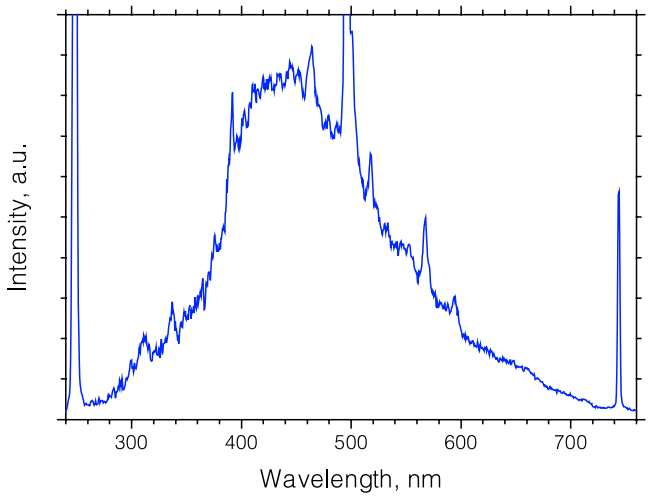

Fig. 4. Plasma emission spectrum from the focal point at a laser power density of ≥4 GW/cm^2 ($\lambda_{exc} = 247.910$ nm). Features at ∼248, ∼496 and ∼744 nm are due to scattered laser radiation.

$OH^*(A)$ molecules are mainly due to ionization in the laser field.

Moreover, as our results show, the major photodissociation product is in the lowest vibrational state $\nu' = 0$. This can be seen from Figure 2c for the following reasons. (i) Transitions from vibrational levels $\nu' \geq 1$ of $OH^*(A)$ are not observed (for example, the 1–0 and 2–1 bands at $\lambda \sim 280$–290 nm), in spite of the fact that at ambient atmosphere conditions the relative intensities of any lines originating from high levels $\nu' \geq 2$ should be higher than when observed under vacuum conditions. This is because high vibrational levels of $OH^*(A)$ predissociate, which strongly decreases their lifetimes and the corresponding fluorescence yield q: $\tau \sim 130$ ns ($\nu' = 2$), and ∼0.20 ns ($\nu' = 3$) [18,19]. In our experiments the fluorescence losses $R_f \gg \tau^{-1}$ are high and the fluorescence yield of long-lived (*e.g.* $\nu' = 0, 1$) and short-lived (*e.g.* $\nu' = 2, 3$) levels no longer depend on τ: $q \propto \tau_A^{*-1}/(R_f + \tau^{-1}) \approx 1/R_f\tau_A^*$. (ii) The shape of the visible continuum is in agreement with the theoretical partial emission spectrum of $H_2O^*(\tilde{C})$ molecules that result in $OH^*(A)$ fragments in the lowest vibrational state [10]. This theoretical curve is shown in Figure 2b by the solid line.

We have attributed the visible fluorescence to a 2-photon excitation process. This has been confirmed by observing the power dependence of this fluorescence signal. The signal obtained by a scan of the observation zone along the focal point of the 15 cm lens is presented in Figure 3. For a Gaussian laser beam the optical power density changes as the distance from the focal point z as $I(z) = I_0 s_f/s$, where s_f and $s = s_f(1 + 4(z/b)^2)$ are the beam waist cross-sections at the focal point and as a general function of z, and b is the confocal parameter. The observed signal will be $I_{fluo} \propto I(z)^k s = I_0^k s_f^k/s^{k-1}$ if k photons participate in the excitation process. The fit of the experimental data gives the photon order of $k = 1.9 \pm 0.4$ and the length of the focal region of $b = 3.6 \pm 1.0$ mm. We conclude that the observed visible fluorescence is therefore due to a 2-photon excitation of the water molecule. In agreement with earlier results by Engel *et al.* [10] the visible band in Figures 2b and 2c centered at ∼420 nm has been assigned to the $\tilde{C}^1B_1 \rightarrow \tilde{A}^1B_1$ fluorescence of molecular water. Moreover, by using the obtained value of b we can estimate the power density at the focal point as ∼2.0 GW/cm^2. At this and at lower power densities, two-UV-photon excitation processes dominate in water vapor fluorescence. At twice this power density plasma begins to appear at the lens focus. This considerably modifies the fluorescence spectrum as shown in Figure 4. As one can see, nitrogen lines may still be visible but the asymmetric continuum due to a transient water emission seems strongly intensified and dominates the spectrum.

An intense vibrational progression with $\omega_{\nu 1} = 2\,200$ cm^{-1} observed in both atmospheric and gaseous nitrogen environments (Fig. 2a) belongs to N_2 radiative transitions directly excited by UV photons. These lines have been assigned to the first negative system of N_2^+ ($B^2\Sigma^+_{u\nu=0,1} \rightarrow X^2\Sigma^+_{g\nu''=0,1,2,3}$ transitions) [20,21]. From energy considerations, the excitation of the $B^2\Sigma_u^+$ state needs at least four UV photons. This hypothesis has been verified by measurements of the fluorescence intensity of the most intense line at ∼390 nm along the optical z-axis using the 15 cm lens. The procedure has been explained above. This scan is included in Figure 3. The fit of the experimental data gives the photon order of $k = 3.3 \pm 0.6$, suggesting that three to four photons are involved in the excitation process of this nitrogen fluorescence. The ionization potential of N_2 is ∼15.6 eV. Three 5.0-eV photons have not sufficient energy to ionize the gas molecules, but may lead to population of high-lying Rydberg states, which are relatively long-lived and can be easily ionized by absorption of a fourth UV photon. Therefore, the fourth photon absorption may not be a limiting process of the excitation scheme, and the effective photon order can be smaller.

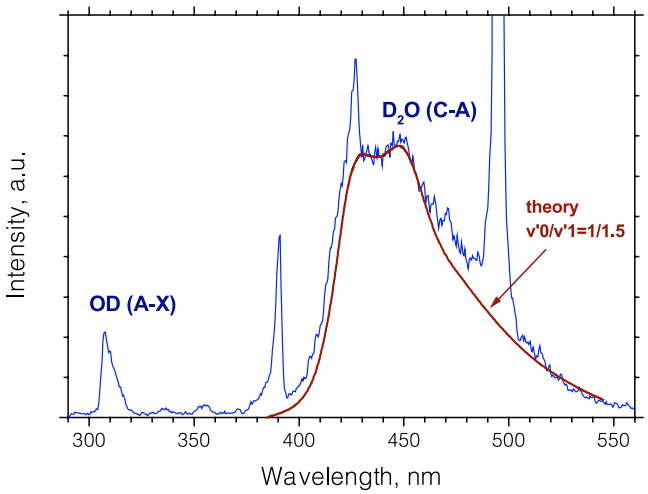

Fig. 5. Fluorescence spectrum of D_2O vapor in the atmospheric environment. The excitation wavelength is 247.545 nm; the laser power density is ~1.0 GW/cm^2. Partial emission cross-section for OD$^*(n0/n1 = 1/1.5)$ vibrational channel from [10] is shown by the solid line.

It is interesting to note that another nitrogen progression, with $\omega_{\nu 2} \approx 1\,250$ cm^{-1}, has been observed in presence of water vapor. This is seen in the difference spectrum presented in Figure 2b. This progression has been tentatively assigned to the second positive system ($C^3\Pi_u \rightarrow B^3\Pi_g$ transitions) of nitrogen [20,21]. Simultaneously, a weak fluorescence has been observed in the spectral range of ~620–640 nm (it is not shown in Fig. 2), which is apparently related to the first positive nitrogen system ($B^3\Pi_g \rightarrow A^3\Sigma_u^+$). Its observation confirms the above assignment. What possible mechanism could explain the $C^3\Pi_u$ state population? Firstly, we have not observed the $C \rightarrow B$ emission in nitrogen atmosphere (Fig. 2a). Apparently, its appearance is due to an energy transfer process involving water molecules. Secondly, because of the spin conservation the excited triplets cannot be directly produced either by photons from the singlet ground state $X^1\Sigma_u^+$ or *via* elastic collisions of excited nitrogen singlet states with surrounding gases. Nor can it be produced in charge exchange reaction between ground state ions $N_2^+(X)$ and $H_2O(\tilde{X})$, because of the lack of energy. We conclude that it is a collisional quenching accompanied by the electron and energy transfer from high lying $N_2^{+*}(E \geq 23.6$ eV) states to the H_2O molecule. These specific states may be excited *e.g.* by a fifth laser photon. The electron recombination reactions $N_2^+ + e + M \rightarrow N_2^*$ may also be responsible for the excited triplet C-state population. If this is a case, H_2O is much more efficient as a third body than N_2.

Similar spectral features to those observed in H_2O have also been found in D_2O vapor. The experimental fluorescence spectrum is presented in Figure 5. These are the UV band due to the $A^2\Sigma^+ \rightarrow X^2\Pi$ transition of OD, produced by predissociation of a heavy water molecule, and a broad visible continuum with a maximum at ~450 nm assigned to the $\tilde{C}^1B_1 \rightarrow \tilde{A}^1B_1$ fluorescence of the predissociating excited state of D_2O. Because of the heavier D-atom, the predissociation rate in $D_2O(\tilde{C})$ is smaller than in $H_2O(\tilde{C})$. As a result, the same fluorescence intensity has been observed in the latter case with one half the pump laser energy. The spectrum lineshape is in a good agreement with the theoretical one assuming that the principal reaction product OD$^*(A)$ is in $\nu' = 0$ and $\nu' = 1$ vibrational states. As in the case of a water vapor at atmospheric temperature and pressure, these intrinsic emissions are accompanied by the fluorescence of N_2^* and N_2^{+*} molecules.

The analysis of the transient fluorescence spectra of H_2O and D_2O molecules in vapor phase allows us to conclude that their perturbations are negligible in atmospheric environment. In the next section we consider the LIF method for analysis of the molecular ground state population. We compare experimental and theoretical excitation spectra of the transient emission assuming a Boltzmann ground state population distribution of vapor phase water molecules.

3.2 $\tilde{C} \rightarrow \tilde{A}$ fluorescence excitation spectra

The theoretical simulation of the two-photon $\tilde{C} \leftarrow \tilde{X}$ absorption of a water molecule was first reported by Ashfold *et al.* [6], before the spectrum had been measured experimentally. More information about the calculation procedure and parameter adjustments was given later in [7,8]. Several important factors should be carefully considered in calculation of the excitation spectra $I_{\rm fluo}(\lambda_{\rm exc})$. Firstly, the $H_2O(\tilde{C})$ molecule heavily predissociates, which increases its individual rotational linewidths and decreases the peak intensities of these lines. Secondly, predissociation to OH(A) fragments occurs through the repulsive $\tilde{B}$ state and the $\tilde{C} \leftrightarrow \tilde{B}$ state coupling rate is J-dependent. Third, the transient fluorescence quantum yield q depends on the level lifetime due to this coupling.

We have carried out theoretical calculations of excitation spectra of H_2O and D_2O molecules using the above-proposed formalism. The absorption belongs to the $3pa_1\tilde{C}^1B_1 \leftarrow 1b_1\tilde{X}^1A_1$ transition and shows a partially resolved rotational structure, which is sensitive to the rotational level population. A water molecule is an asymmetric rotor with rotational constants $(A > B > C)$ in the ground and excited states of $\tilde{X}$(27.8778; 14.5092; 9.2869) cm^{-1} and of $\tilde{C}$(25.67; 12.55; 8.55) cm^{-1}, respectively. The $\tilde{C} \leftarrow \tilde{X}$ electronic transition energy is $T_0 = 80\,624.7$ cm^{-1} [6,22]. Corresponding spectroscopic constants of the D_2O molecule used in our calculations are: $\tilde{X}$(15.3846; 7.2716; 4.8458) cm^{-1}, $\tilde{C}$(14.64; 6.31; 4.42) cm^{-1} and $T_0 = 80\,751.9$ cm^{-1} [22]. A rotational level classification J_{K_a,K_c} (K_a and K_c are J-projections on the molecular axes) has been used for both ground and excited states and the corresponding term energies have been calculated in accordance with [23]. The linewidth is defined as $\Delta\nu = F\Delta\nu_0$, where $F = 1 + c\langle J_a'^2\rangle + \beta$. The first and the second terms in F correspondingly represent

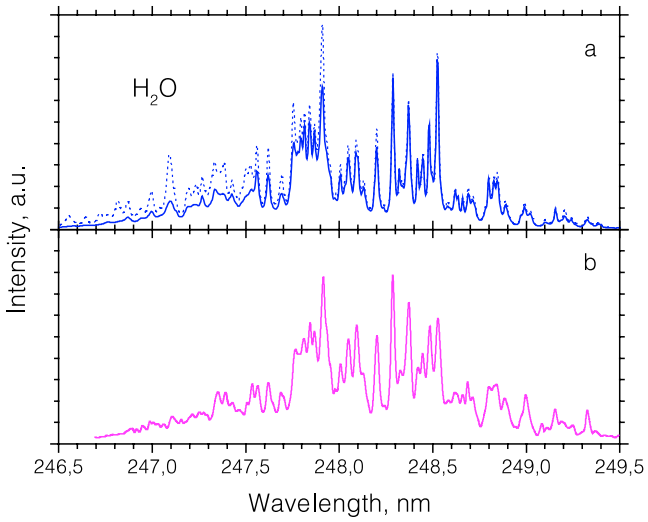

Fig. 6. Theoretical (a) and experimental (b) fluorescence excitation spectra of the H_2O molecule. The theoretical spectrum was calculated with adjusted linewidth parameters and is shown in (a) as a solid line. The laser power density is ~2.0 GW/cm^2, room temperature is 300 K.

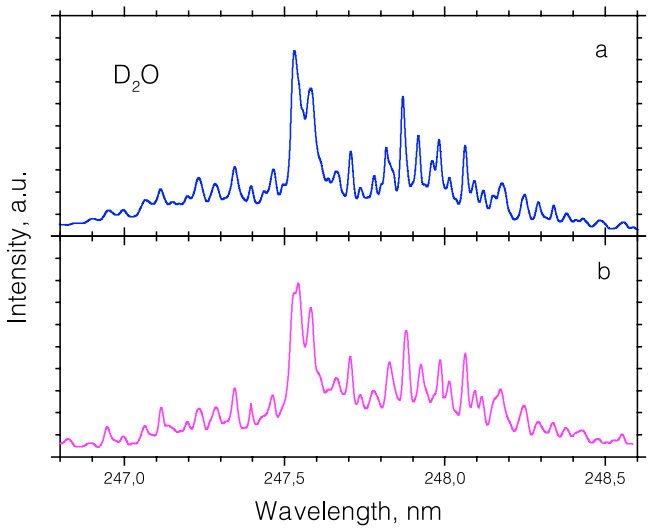

Fig. 7. Theoretical (a) and experimental (b) fluorescence excitation spectra of the D_2O molecule. The laser power density is ~1.0 GW/cm^2 and room temperature is 300 K.

homogeneous and heterogeneous contributions. The third term in F contains the lifetime (β_1) and the ionization (β_2) contributions to the predissociation rate. The mean square projection of the rotational angular momentum on the a-molecular axis, $\langle J_a'^2 \rangle$, has been used instead of $K_a'^2$ because K_a' cannot be considered as a good quantum number for an asymmetric rotor. The relative $J'_{K_a',K_c'} \leftarrow J''_{K_a'',K_c''}$ peak heights are defined as $h = F^{-2}$ because of the linewidth and q contributions. The following constants $\Delta\nu_0$ and c in the above formula were used: 2.1 cm^{-1} and 0.35 for H_2O and 1.0 cm^{-1} and 0.50 for D_2O molecules [6–8]. The laser spectral linewidth of $\Delta\omega = 0.2$ cm^{-1} and the natural radiative linewidth (the β_1 contribution) have been neglected in our calculations. Because of a rather strong laser energy density at the focal point, we could not neglect the ionization (factor β_2), however. An estimate of this factor was made by observation of the experimental shape of the $J'_{K_a',K_c'} \leftarrow J''_{K_a'',K_c''}$ lines of the $\tilde{C}$ state with low K_a-numbers. A well-separated spectral line at 248.287 nm was used. It terminates on the 2_{02} level with a very small contribution from the heterogeneous predissociation ($\langle J_a'^2 \rangle = 0.025$). The best fit to this lineshape is obtained with the parameter $\beta_2^{H_2O} = 1.2 \pm 0.2$. Finally, the Boltzmann population of rotational levels at room temperature of 300 K was assumed. The theoretical spectrum of the H_2O molecule thus calculated is shown by the dotted lines in Figure 6a.

Experimentally, two-photon excitation spectra of H_2O and D_2O molecules were measured at ambient atmospheric conditions and at $T = 300$ K. Fluorescence was observed from the focal point through a filter-monochromator fixed at the visible continuum. The experimental curves are shown by solid lines in Figures 6b and 7b. Below we compare experimental results with the theory.

Comparison of the two spectra in Figure 6 for H_2O shows an agreement in the long-wavelength region, $\lambda \geq 247.72$ nm. Although, almost all characteristic peaks appear in the short-wavelength region ($\lambda \leq 247.72$ nm) of the measured spectrum, those intensities are strongly attenuated. Especially strong attenuation begins at $\lambda \leq 247.30$ nm (5.0139 eV). Apparently, this is not an effect of the environmental gases. As it is seen from the experimental spectrum of D_2O measured at the same conditions (see in Fig. 7b), no such difference between the experiment and the theory has been observed. How this can be explained?

Earlier, Ashfold *et al.* [6] discussed the problem of line intensities in the multi-photon ionization (3+1 MPI) spectra of the H_2O molecule. It has been found that predissociation of the intermediate excited state $\tilde{C}^1B_1$ increases more than linearly with the quantum number K_a'. Two parameterizations model have been originally suggested: $F = 1 + cK_a'^2$ and $F = \exp(\gamma K_a'^2)$ [1]. The first one has been later used and rationalized in terms of the relevant Coriolis coupling matrix elements that provide the necessary $C \rightarrow B$ transfer. However, this model has been explicitly considered in a partial range of the relevant rovibronic $\tilde{C} \leftarrow \tilde{X}$ transitions (practically, to levels having $K_a' \leq 2$), since transitions to higher levels having $K_a' > 2$ are not discernible in the tuning range of the KrF laser (247.8–248.8 nm). In the present work a complete fluorescence excitation spectrum of the $\tilde{C}^1B_1 \leftarrow \tilde{X}^1A_1$ two-photon transition is measured for the first time. The results show that the major features in the H_2O excitation spectra at $\lambda \leq 247.72$ nm (although being weak) belong to fluorescence from rotational levels with $K_a' = 3$–6. Those observations permit comparing the two earlier proposed models. The best fit of the low-energy part of the

[1] We note that these models distinguish for high K_a'-levels; for low K_a'-levels they practically result in the same representation, using $c = \gamma$.

spectrum ($\lambda = 247.8-248.8$ nm) using the first parabolic model (shown by a dotted curve in Fig. 6a), disagrees the high-energy part of the spectrum, $\lambda < 247.8$ nm. On the other hand, the exponential parameterization modified as $F = \exp(\gamma\langle J_a'^2\rangle)$ is clearly preferred, as it succeeds reproducing the experimental spectrum. This result is shown in Figure 6a by a solid curve. To improve reproduction of the total experimental spectrum we have increased the constant $\gamma_{H_2O} = 0.4$ from that previously suggested ($\gamma = 0.2$). Although some disagreement may exist, this approach results in a generally better representation of experimental data, as the observed nonlinearity in the $F(K_a')$ behavior for high J-levels may be stronger than quadratic.

In analogy with H_2O, the same tendency was observed in D_2O and the second model with $F = \exp(\gamma K_a'^2)$ shows good results with $\gamma_{D_2O} = 0.25$. The calculated spectrum is shown in Figure 7a. This γ-value is also larger than that proposed earlier ($\gamma = 0.12$). Moreover, the lineshape parameter due to ionization phenomena $\beta_2^{D_2O} = 3.0 \pm 0.5$ was also obtained in these calculations (for our experimental conditions). Comparison between the experiment and the theory allows a simple analysis of the set of rotational constants of the excited $\tilde{C}^1B_1$ state. From high-resolution VUV spectra of D_2O, Johns [22] has obtained values $\tilde{C}(14.74; 6.31; 4.28)$ cm^{-1} (s1), which were subsequently corrected as $\tilde{C}(14.64; 6.31; 4.42)$ cm^{-1} (s2). Recently, Ashfold *et al.* [6] used the first set of the data in calculations of the multiphoton $\tilde{C} \leftarrow \tilde{X}$ transition. We were unable to fit our experimental spectra with the s1 constants. Although, low-J lines are in a reasonable agreement with such calculations, high-J lines are not. The strongest deviation $\sim$10 cm^{-1} appears for the strongest spectral feature at $\sim$247.53 nm. This line cannot be associated with a unique transition, but belongs in fact, to a group of transitions to the high-lying J'_{K_a,K_c} rotational levels with $J' = 7-10$. This spectral range has never before been observed; and so comparison with other experiments is not possible. Our use of the s2 constants results in an excellent agreement with the experiment.

The obtained experimental results allow a comparison of two-photon $\tilde{C} \leftarrow \tilde{X}$ excitation efficiencies η of D_2O and H_2O molecules. The experimental geometry did not change during these experiments. Therefore, we can use the $N_2^+\ B^2\Sigma^+_{u\nu=0} \rightarrow X^2\Sigma^+_{g\nu''=0,1}$ fluorescence for a normalization of the visible fluorescence spectra: $I_{N_2^+} \propto I_{H_2O/D_2O} I_L^{1.4}$. The obtained ratio is $\eta_{D_2O}/\eta_{H_2O} \approx 4.1$, which corresponds to the excitation in spectral maxima at 247.545 nm (D_2O) and 247.915 nm (H_2O). One more remark concerns a difference between β_2-values obtained from the excitation spectra of H_2O and D_2O molecules. Apparently, a 2.5-times larger contribution to the spectral linewidth indicates a stronger ionization of D_2O then H_2O molecules. Both these effects (higher fluorescence efficiency and larger linewidth in D_2O respectively to that in H_2O) may be related to the excited-state lifetime, which should be considerably longer in D_2O. Estimates based on $K_a' = 0$ level linewidth measurements give lifetimes of 2.5 ps and 6 ps for the $\tilde{C}^1B_1$ state of H_2O and D_2O molecules [6], respectively.

4 Conclusions

Transient visible fluorescence of the heavily predissociated excited $\tilde{C}^1B_1$-state of H_2O and D_2O molecules has been measured at ambient atmospheric conditions. Complete two-photon fluorescence excitation spectra between 245 and 250 nm were measured for the first time, using a narrow-band tunable OPO laser, and compared with theory. Principal excited-state products of $N_2^+(B)$, $OH(A)/OD(A)$, $H_2O(\tilde{C})/D_2O(\tilde{C})$ were observed. It is shown that excited ions $N_2^+(B)$ appear at the focal point due to a four-photon absorption. Moreover, a weak vibrational progression assigned to the second positive system of N_2 was observed, which seems to be due to the energy and charge transfer in $N_2^{+*} + H_2O$ collisions. Neither collisions with atmospheric gases nor ionization phenomena at laser power density below 2 GW/cm^2 do perturb the isolated molecular spectra. The comparison of experimental and theoretical excitation spectra of both H_2O and D_2O molecules shows that the predissociation rate of J'_{K_a,K_c} rotational levels increases with the rotational quantum number $K_a' > 2$ faster than $K_a'^2$.

We are particularly grateful to the MENR of France for the financial support of this work. Discussions with Carl D. Scott and Colm Mc Ginley are highly acknowledged.

References

1. O. Dutuit, A. Tabche-Fouhaile, I. Nenner, H. Frohlich, P.M. Guyon, J. Chem. Phys. **83**, 584 (1985)
2. V. Engel, V. Staemmler, R.L. Vander Wal, F.F. Crim, R.J. Sension, B. Hudson, P. Andresen, S. Henning, K. Weide, R. Schinke, J. Phys. Chem. **96**, 3201 (1992)
3. M. Chergui, N. Schwentner, V. Stepanenko, Chem. Phys. **187**, 153 (1994)
4. P. Grtler, V. Saile, E.E. Koch, Chem. Phys. Lett. **51**, 386 (1977)
5. M.N.R. Ashfold, Mol. Phys. **58**, 1 (1986)
6. M.N.R. Ashfold, J.M. Bayley, R.N. Dixon, Chem. Phys. **84**, 35 (1984)
7. A. Hodgson, J.P. Simons, M.N.R. Ashfold, J.M. Bayley, R.N. Dixon, Mol. Phys. **54**, 351 (1985)
8. G. Meijer, J.J. ter Meulen, P. Andresen, A. Bath, J. Chem. Phys. **85**, 6914 (1986)
9. R.N. Dixon, J.M. Bayley, M.N.R. Ashfold, Chem. Phys. **84**, 21 (1984)
10. V. Engel, G. Meijer, A. Bath, P. Andersen, R. Schinke, J. Chem. Phys. **87**, 4310 (1987)
11. P. Andresen, A. Bath, W. Gröger, H.W. Lülf, G. Meijer, J.J. ter Meulen, Appl. Opt. **27**, 365 (1988)

12. A. Kanaev, L. Museur, T. Laarman, S. Monticone, M.C. Castex, K. von Haeften, T. Möller, J. Chem. Phys. **115**, 10248 (2001)
13. C. Fotakis, C.M. McKendrick, R.J. Donovan, Chem. Phys. Lett. **80**, 598 (1981)
14. L.C. Lee, L. Oren, E. Phillips, D.L. Judge, J. Phys. B: At. Mol. Phys. **11**, 47 (1978)
15. J.H. Brophy, J.A. Silver, J.L. Kinsey, Chem. Phys. Lett. **28**, 418 (1974)
16. A.E. Bailey, D.E. Heard, D.A. Henderson, P.H. Paul, Chem. Phys. Lett. **302**, 132 (1998)
17. P.H. Paul, J.L. Durant, J.A. Gray, M.R. Furlanetto, J. Chem. Phys. **102**, 8378 (1995)
18. J. Brzozowski, P. Erman, M. Lyyra, Phys. Scripta **17**, 507 (1978)
19. D.R. Yarkony, J. Chem. Phys. **97**, 1838 (1992)
20. G. Herzberg, *Molecular spectra and molecular structure. I. Spectra of diatomic molecules*, 2nd edn. (D. van Nostrand Company, N.Y., 1966)
21. A. Lofthus, P.H. Krupenie, J. Phys. Chem. Ref. Data **6**, 113 (1977)
22. J.W.C. Johns, Can. J. Phys. **41**, 209 (1963); *ibid.* **49**, 944 (1971)
23. G.B. King, R.M. Hainer, P.C. Cross, J. Chem. Phys. **11**, 27 (1943)